Passive synchronization of all-fiber lasers through a common saturable absorber

M. Zhang,[1,*] E. J. R. Kelleher,[1] A. S. Pozharov,[2] E. D. Obraztsova,[2] S. V. Popov,[1] and J. R. Taylor[1]

[1]*Femtosecond Optics Group, Department of Physics, Imperial College London, London, SW7 2AZ, U. K.*

[2]*A. M. Prokhorov General Physics Institute, 38 Vavilov Street, 119991, Moscow, Russia*

**Corresponding author: m.zhang10@imperial.ac.uk*

Received June 3, 2011; revised August 24, 2011; accepted September 12, 2011;
posted September 13, 2011 (Doc. ID 148732); published October 5, 2011

We present the synchronization of two all-fiber mode-locked lasers, operating at 1.0 μm and 1.54 μm, coupled through the use of a shared single-wall carbon nanotube absorber. Both lasers operate in the soliton-regime, achieving a synchronized repetition rate of 13.08 MHz. The broadband absorption range of the single-wall carbon nanotubes allows the stable mode-locking behavior at 1 μm and 1.5 μm. The nonlinear coupling effects between two energy states of the carbon nanotube absorber result in stable synchronized pulses for hours of operation, with a large cavity mismatch of 1400 μm. © 2011 Optical Society of America

OCIS codes: 140.3500, 140.3510, 140.4050, 320.7090.

Passively mode-locked fiber laser sources using saturable absorbers, are a mature technology and widely deployed in a broad range of applications for generating ultrashort pulses because of their compactness, stability, and low cost. Rare-earth-doped fiber gain media, such as ytterbium (Yb) and erbium (Er), offer emission around 1.06 μm and 1.55 μm, respectively [1–3]. More recently, bismuth-doped fiber amplifiers (BiDFAs) have received attention because they provide fluorescence in a band (1.1–1.4 μm) not covered by rare-earth technologies [4]. In some applications, for example pump-probe processes, Raman scattering spectroscopy [5], and difference-frequency mixing, tunable single wavelength sources are not sufficient for the requirements; thus synchronized two-wavelength mode-locked lasers with a locked repetition rate have emerged and have been demonstrated using different methods: active synchronization [6,7] that applies electronic feedback to control the cavity length, active-passive hybrid synchronization [8] and passive synchronization [9], where the nonlinear interaction of the two beams promotes coupling. The relative timing jitter, which currently has the most advanced reported results of attoseconds [7,8], provides an important metric for the stability of the systems synchronization and is required for optimal performance in the majority of applications. Previous reports have shown that solid-state passively synchronized laser systems, using cross-phase modulation (XPM), result in low timing jitter and large cavity mismatch [10]. Compared with solid-state lasers, fiber lasers offer the advantages of environmental stability, compactness, and higher efficiency. Recently, the passive synchronization of fiber lasers has been achieved in a number of ways: using XPM [11–14] in a common fiber length or using a shared saturable absorber in a master-slave configuration [15], where the master injection mode-locks the slave. In addition, saturable absorbers have been used to stabilize mode-locking through direct pump modulation [16]. Here we present a synchronized all-fiber system using a broadband single-wall carbon nanotube (SWNT) saturable absorber for mode-locking as well as enabling broad wavelength range, two-color synchronization.

In this Letter, a passive synchronization has been demonstrated for the first time, to our knowledge, between an Er- and Yb-laser by sharing a broadband SWNT saturable absorber. This element was constructed as a polymer (carboxymethylcellulose) thin film (with thickness about 10 μm) with embedded individual SWNTs [17]. Both lasers operated in the soliton-regime, achieving a synchronized repetition rate of 13.08 MHz. The broadband absorption range of the SWNTs ensures the stable mode-locking behavior at 1 μm and 1.5 μm. The nonlinear coupling effects between two energy states of a SWNT result in the stable synchronization of pulses generated in the two-color laser for several hours and a large tolerable cavity length mismatch of ~1400 μm.

The configuration of the two-color all-fiber laser is shown in Fig. 1(a), with the top and bottom parts presenting the Er-laser and Yb-laser, respectively.

In the Er-laser, a fiber amplifier module providing a noise seed and amplification in a band around 1.55 μm was followed by an inline optical isolator. The output signal was delivered through a 50:50 fused-fiber coupler, and a polarization controller was added to adjust the polarization state within the cavity, but was not fundamental to the mode-locking action. The cavity length of

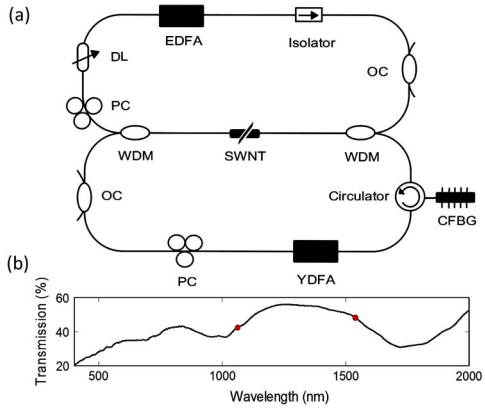

Fig. 1. (Color online) (a) Schematic of the two-color all-fiber mode-locked laser. EDFA, erbium doped fiber amplifier; OC, output coupler; PC, polarization controller; WDM, wavelength division multiplexer (1.55/1.06 μm); YDFA, ytterbium doped fiber amplifier; CFBG, chirped fiber Bragg grating. (b) Linear transmission spectrum of the carbon nanotube film used in the two-color mode-locked laser.

the Er-laser could be changed by a maximum of 9 cm through a fiber-pigtailed optical delay line, with a corresponding optical delay of 300 ps. The Er-laser cavity contained ~15 m of single mode fiber (SMF28), resulting in the laser operating in the soliton-regime. The Yb-laser, one-half of the two-color laser, was constructed from a fiber amplifier module generating the noise seed and amplification around 1.06 μm, a 20% output fused-fiber coupler, and a PC. A polarization independent inline fiber circulator was employed to incorporate a chirped Bragg grating, providing a negative dispersion of $-21.6\,\mathrm{ps}^2$, and ensuring unidirectional propagation.

Both lasers shared a transparent carboxymetylcellulose film with homogeneously embedded individual SWNTs [17], embedded by two 1060/1550 wavelength division multiplexers (WDM) into each individual cavity. The SWNT saturable absorber device provides intensity dependent loss to initiate mode-locking. SWNTs were synthesized by an arc-discharge technique [18]. The linear transmission of the SWNT saturable absorber is plotted in Fig. 1(b), showing two prominent absorption features at 1.8 μm and 1.0 μm, corresponding to the S_1 and S_2 electronic transitions in the density of states. It was recently shown that mode-locking could be achieved using the S_2 transition [17], diversifying the operation range of SWNT devices and used here to synchronize the two-color laser. The red dots in Fig. 1(b) indicate the points on the linear transmission curve where the Yb and Er lasers operate, with ~40% (S_2) and ~50% (S_1) linear absorption, respectively. The nonlinear response of this device was measured previously in [19]. Measurements of the pulse repetition rate were carried out with a fast photodiode connected to a radio frequency analyzer (RF analyzer). Stable, self-starting mode-locking was obtained in both lasers independently using the same SWNT device. In the nonsynchronized state, the spectral and temporal intensity of the Er-laser pulses were maintained while the cavity length was adjusted through the delay line. The systems behaved like two independent lasers. When the repetition rate of the Er-laser was finely tuned using the delay line to twice the value of the Yb-laser's, a passive synchronization was achieved. As the pump power of the Yb-laser varied, two modes of synchronization were observed: either the repetition rate was locked at the fundamental frequency or the second cavity harmonic frequency, with the latter observed as the pump power increased. When synchronized at the repetition rate of both their fundamental frequency, the radio frequency spectra were measured by an RF analyzer, with the value of 6.54 MHz and 13.08 MHz in Yb-laser and Er-laser, respectively. The corresponding single pulse energy was 1.9 pJ for the Yb-laser and 15 pJ for the Er-laser, assuming all the energy is contained within the body of the pulse. The pulse width in the Er-laser, measured using intensity autocorrelation, was 2.1 ps fitted with a sech^2 pulse shape and plotted in Fig. 2(a). The spectrum was [Fig. 2(c)] centered at 1535.48 nm, with a full width at half-maximum (FWHM) of 1.48 nm. Figure 2(b) shows the autocorrelation of the Yb-laser with a pulse width of 6.1 ps and a corresponding spectral FWHM 0.24 nm [centered at 1067.1 nm, Fig. 2(d)]. To obtain the higher harmonic frequencies of the synchronized laser, the output pulses from both lasers were

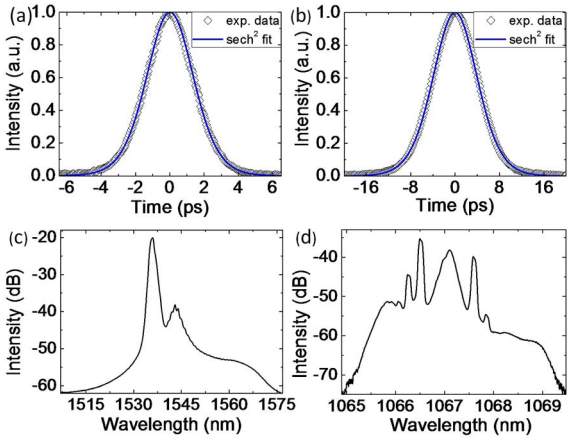

Fig. 2. (Color online) Intensity autocorrelations of (a) Er-laser and (b) Yb-laser, with a sech^2 fitting, and the corresponding optical spectra of (c) an Er-laser and (d) a Yb-laser.

injected into a 1060/1550 WDM, and Fig. 3(a) shows the measured frequency components detected from the output port of the WDM. Figure 3(b) shows the repetition rates of both lasers as a function of the cavity length tuning of the Er-laser through the variable delay line. In the fundamental mode of the synchronized operation, where there is only one mode-locked pulse inside the cavities, both lasers remained at the repetition frequency imposed by the Yb-laser and obtained for the maximum detuned frequency of 1200 Hz, corresponding to a tolerable cavity length mismatch of ~1400 μm.

It is noted that the transition from the nonsynchronized mode to the synchronized regime described above does not modify the pulse parameters within experimental accuracy; however, we did observe a small decrease (~5%) in the threshold power of both lasers. We believe that this could be attributed to the relaxation dynamics of the S_2 transition of the saturable absorber device, excited by a 1 μm photon: the electron in the CNT matrix nonradiatively decays via the S_1 level, coupling the saturable losses to the 1.55 μm transition. This model of saturable decay of the S_2 transition has been illustrated by photoluminescence measurements in [20] that show only a strong signal at the corresponding S_1 transition. Thus, in the synchronized mode, the S_1 state is occupied and saturated by both lasers and results in a decrease of

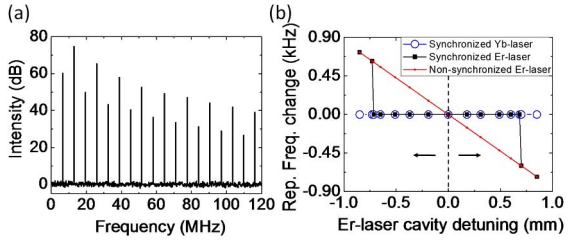

Fig. 3. (Color online) (a) Higher harmonic frequencies of the synchronized two-color pulses, on a span of 120 MHz, with a resolution of 3 KHz. (b) Repetition rates of the synchronized Yb- (blue round) and the Er-laser (black square) under different cavity length mismatches. The synchronized repetition rate is 13.08 MHz and twice the repetition rate of the Yb-laser is plotted. The diagonal line (red triangle) presents the cavity-length-dependent repetition rates of the nonsynchronized Er-laser.

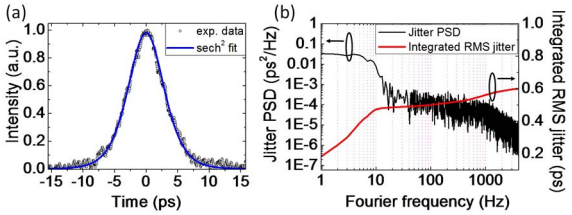

Fig. 4. (Color online) (a) Cross-correlation trace from the two synchronized all-fiber mode-locked lasers. (b) Sum-frequency generation intensity-noise power spectral density (PSD) and integrated timing jitter of the synchronized lasers.

threshold. Different from [11–14], we do not expect XPM to contribute to the synchronized operation because of low intracavity peak powers and a short shared interaction length; the nonlinear coupling effects between the S_1 and S_2 states of the SWNT support the synchronization.

To further qualify the synchronization, the timing jitter between the two lasers was measured by cross-correlation technique [21]. The output pulses of the Er- and Yb- laser were amplified to 2.84 mW and 6.03 mW, corresponding to 217.2 pJ and 921.6 pJ, by an Er-amplifier and a Yb-amplifier, respectively. By adjusting the variable delay line in one arm of the cross-correlation, the cross-correlation trace was obtained and recorded on an oscilloscope, with the FWHM of 6.5 ps, shown in Fig. 4(a). In order to achieve the timing jitter between the two synchronized lasers, the half-maximum intensity of the cross-correlation trace was recorded with 8000 points in one second, corresponding to the Nyquist frequency of 4 kHz.

The calibrated power spectral density and the integrated root mean square (RMS) timing jitter of 600 fs, in a Fourier frequency range from 1 Hz to 4 kHz, are shown in Fig. 4(b). Beyond 1 kHz, the jitter power spectral density (PSD) decays while the integrated RMS timing jitter appears to saturate (~530 fs RMS jitter from 1 Hz to 1 kHz), indicating that the jitter was mainly contributed by lower frequency noise. Compared to previous reports [22] the jitter is large. Reducing the duration of the pulses will reduce the degree of pulse jitter and this will be the subject of a future publication.

In conclusion, we have presented the synchronization of an Yb- and Er- fiber laser by sharing a SWNT saturable absorber, for the first time, to the best of our knowledge. A cavity mismatch tolerance of ~1400 μm was achieved and the RMS timing jitter was 600 fs from 1 Hz to 4 kHz. This all-fiber synchronization by sharing the common saturable absorber could be applied to other two-color sources for a simple and compact, passive solution.

The Femtosecond Optics Group is supported by studentships from the U. K. Engineering and Physical Sciences Research Council and by the Royal Society. J. R. Taylor is a Royal Society Wolfson Research Merit Award holder. S. V. Popov is a Royal Society Industry Fellow. The GPI RAS laboratory is grateful for support by Russian Foundation for Basic Research (RFBR) projects 10-02-00792 and 11-02-92121.

References

1. O. G. Okhotnikov, L. Gomes, N. Xiang, T. Jouhti, and A. B. Grudinin, Opt. Lett. **28**, 1522 (2003).
2. R. E. Kennedy, S. V. Popov, and J. R. Taylor, Opt. Lett. **31**, 167 (2006).
3. C. J. S. de Matos, R. E. Kennedy, S. V. Popov, and J. R. Taylor, Opt. Lett. **30**, 436 (2005).
4. E. J. R. Kelleher, J. C. Travers, K. M. Golant, S. V. Popov, and J. R. Taylor, IEEE Photon. Technol. Lett. **22**, 793 (2010).
5. F. Ganikhanov, S. Carrasco, X. S. Xie, M. Katz, W. Seitz, and D. Kopf, Opt. Lett. **31**, 1292 (2006).
6. T. R. Schibli, J. Kim, O. Kuzucu, J. T. Gopinath, S. N. Tandon, G. S. Petrich, L. A. Kolodziejski, J. G. Fujimoto, E. P. Ippen, and F. X. Kaertner, Opt. Lett. **28**, 947 (2003).
7. J. Kim, J. A. Cox, J. Chen, and F. X. Kärtner, Nat. Photon. **2**, 733 (2008).
8. D. Yoshitomi, Y. Kobayashi, H. Takada, M. Kakehata, and K. Torizuka, Opt. Lett. **30**, 1408 (2005).
9. C. Fürst, A. Leitenstorfer, and A. Laubereau, IEEE J. Sel. Top. Quantum Electron. **2**, 473 (1996).
10. D. Yoshitomi, Y. Kobayashi, M. Kakehata, H. Takada, K. Torizuka, T. Onuma, H. Yokoi, T. Sekiguchi, and S. Nakamura, Opt. Lett. **31**, 3243 (2006).
11. M. Rusu, R. Herda, and O. G. Okhotnikov, Opt. Lett. **29**, 2246 (2004).
12. W.-W. Hsiang, C.-H. Chang, C.-P. Cheng, and Y. Lai, Opt. Lett. **34**, 1967 (2009).
13. M. Rusu, R. Herda, and O. G. Okhotnikov, Opt. Express **12**, 4719 (2004).
14. M. Yan, W. Li, Q. Hao, Y. Li, and H. Zeng, Opt. Lett. **34**, 2018 (2009).
15. T. Walbaum, M. Löser, P. Gross, and C. Fallnich, Appl. Phys. B **102**, 743 (2011).
16. M. Guina and O. G. Okhotnikov, Appl. Phys. B **75**, 127 (2002).
17. A. I. Chernov, E. D. Obraztsova, and A. S. Lobach, Physica Status Solidi. B **244**, 4231 (2007).
18. E. D. Obraztsova, J.-M. Bonard, V. L. Kuznetsov, V. I. Zaikovskii, S. M. Pimenov, A. S. Pozharov, S. V. Terekhov, V. I. Konov, A. N. Obraztsov, and A. P. Volkov, Nanostruct. Mater. **12**, 567 (1999).
19. J. C. Travers, J. Morgenweg, E. D. Obraztsova, A. I. Chernov, E. J. R. Kelleher, and S. V. Popov, Laser Phys. Lett. **8**, 144 (2011).
20. S. M. Bachilo, M. S. Strano, C. Kittrell, R. H. Hauge, R. E. Smalley, and R. B. Weisman, Science **298**, 2361 (2002).
21. T. Miura, H. Nagaoka, K. Takasago, K. Kobayashi, A. Endo, K. Torizuka, M. Washio, and F. Kannari, Appl. Phys. B **75**, 19 (2002).
22. C. Zhou, Y. Cai, L. Ren, P. Li, S. Cao, L. Chen, M. Zhang, and Z. Zhang, Appl. Phys. B **97**, 445 (2009).